# Inelastic scattering and excitation of $^6$Li

M. F. Vineyard,* J. Cook,† and K. W. Kemper
*Department of Physics, Florida State University, Tallahassee, Florida 32306*
(Received 25 September 1984)

Differential cross sections for elastic and inelastic $^6$Li scattering from $^{12}$C at $E_{c.m.}=16$ and 20 MeV, and scattering from $^{16}$O at 18.7 MeV were measured out to $\theta_{c.m.}\approx 170°$. Also by scattering $^{12}$C and $^{16}$O from $^6$Li, the inelastic cross sections for the excitation of the $3^+$ (2.18 MeV) and the $2^+$ (4.31 MeV) states of $^6$Li and an estimate of the continuum inelastic cross sections of $^6$Li were determined. The inelastic data were analyzed using the distorted-wave Born approximation and coupled-channels techniques with folded real and phenomenological imaginary form factors, with the deformations derived from electron scattering. The inelastic data are well described. Coupled-channels effects due to the $3^+$ state of $^6$Li were found to play an important role in the scattering. The inclusion of the $3^+$ state in the coupled-channels calculations reduced the discrepancy in the normalization of the real double-folded potential between $^6$Li and other heavy-ion projectiles, and the imaginary potential became weaker in the surface region. The present results show that $L=2$ coupling in the elastic scattering is very important and that the source can be a state in either the projectile, the target, or both.

## I. INTRODUCTION

Recently, considerable success[1] has been achieved in obtaining microscopic optical potentials for nuclear scattering beginning with the $M3Y$ nucleon-nucleon effective interaction.[2] However, success in describing the scattering of $^6$Li, $^7$Li, and $^9$Be projectiles has been possible only with a significant reduction in the strength of the potential.[1] Since these nuclei are weakly bound ($\sim$2 MeV), attempts to understand the need for the reduction in the strength of the microscopic potential have focused on coupling to the breakup channels.[3] At present, very little data exists and only a few theoretical calculations have been performed to investigate the effect of projectile breakup on the elastic scattering.

Depending upon the projectile energy, two different breakup modes may be expected. For projectile energies well below the Coulomb barrier, the projectile may be excited by the electromagnetic field between the incident channel nuclei. If the projectile excited states are above the threshold for particle emission, the projectile will in most cases sequentially breakup beyond the influence of the target's nuclear field.[4,5] However, at high energies, a projectile incident on the peripheral region of the target nucleus might be expected to undergo a rapid nonsequential breakup, i.e., direct breakup.[5,6] For a projectile with an intermediate energy, it should be possible to identify both breakup modes.

Previous studies in projectile breakup of $^6$Li and $^7$Li have not yielded conclusive information about the breakup mechanisms. A recent investigation[5] of 70 MeV $^7$Li($\alpha$ + t) breakup on $^{12}$C and $^{208}$Pb targets, found that the breakup of $^7$Li on the $^{12}$C target, which at 70 MeV is well above the Coulomb barrier, is predominantly sequential, i.e., proceeding through the 4.63 MeV state of $^7$Li, while the breakup of $^7$Li on $^{208}$Pb has both the sequential and direct components. A group at Heidelberg[7] has studied the breakup of $^6$Li in the field of the heavy target nuclei $^{118}$Sn and $^{208}$Pb at energies around the Coulomb barrier, and found the dominant process to be the sequential breakup $^6$Li*($\alpha$ + d) proceeding through the 2.18 MeV ($J^\pi=3^+$) state in $^6$Li. Until now, there has been no data available for the breakup of $^6$Li on lighter targets at energies above the Coulomb barrier.

The main thrust of this work is concerned with the investigation of the effects of coupling to the discrete unbound states of $^6$Li on the elastic scattering. Proton and $\alpha$ scattering by $^6$Li shows its 2.18 MeV $3^+$ state to be strongly excited, and it is possible that coupled-channels effects due to this state play an important role in $^6$Li scattering. To investigate this, angular distributions for the excitation of states in both nuclei have been measured for the $^6$Li + $^{12}$C and $^6$Li + $^{16}$O systems at energies above the Coulomb barrier. These are the first measurements of the predominantly nuclear excitation of the discrete unbound states of $^6$Li in a heavy-ion collision.

In this paper, the inelastic data are analyzed in the distorted-wave Born approximation (DWBA) and coupled-channels (CC) frameworks. Section II describes the experimental procedure used to measure the cross sections. The folded form factors that were employed are described in Sec. III. In the DWBA calculations (Sec. IV) the previously determined folded potentials were used. The CC analysis (Sec. V) was performed to determine the extent to which coupling to different excited states alters the potentials, in particular the normalization of the real folded potential. The results are discussed in Sec. VI, and the conclusions presented in Sec. VII.

## II. EXPERIMENTAL METHOD

Since the experimental details have been discussed in detail in earlier publications[8,9] only a brief description will be presented here. The forward-angle data were taken by

 

scattering $^6$Li from natural C and $SiO_2$ targets of thicknesses between 100 and 300 $\mu g/cm^2$. The $^6$Li targets, used for determining the excitation of the states in $^6$Li by $^{12}$C and $^{16}$O, were enriched to 99.3% and deposited on Formvar backings. Their thicknesses were in the range of 30—70 $\mu g/cm^2$. The beams used in these studies were produced in an inverted sputter source and accelerated by the Florida State University (FSU) super FN tandem Van de Graaff. The scattered particles were detected in surface barrier $\Delta E \times E$ counter telescopes and particle identification of the reaction products was done on line. For the $^{16}$O and $^{12}$C bombardments of the $^6$Li targets, both the scattered $^{16}$O and $^{12}$C and recoil $^6$Li products were detected. The recoil $^6$Li nuclei allowed the large-angle portion of the angular distributions for the excited states in $^{16}$O and $^{12}$C to be measured relatively easily.

The $^6$Li + $^{12}$C data were taken at two energies to investigate the energy dependence of the scattering for this system. The c.m. energy of 16 MeV was chosen to investigate the existence of an anomaly which has been reported[10,11] at the nearby c.m. energy of 15.2 MeV. The c.m. energy of 20 MeV was chosen to be close to previously measured large angle data at 20.4 MeV,[12] so that any rapid change in the angular distributions at large angles would be found. Angular distributions were obtained for the excitation of the $3^+$, 2.18 MeV and $2^+$, 4.31 MeV states of $^6$Li, and the $2^+$, 4.44 MeV, $0^+$, 7.65 MeV, and $3^-$, 9.64 MeV states of $^{12}$C.

A typical spectrum from the $^{12}$C + $^6$Li reaction is shown in Fig. 1(a). Spectra were also taken on a $^{12}$C target and a $SiO_2$ target at each angle so that the location in the spectra and the yields from these contaminants could be determined. Typical spectra taken on the $^{12}$C and $SiO_2$ targets are shown in Figs. 1(b) and (c), respectively. It can be seen in the spectrum from the $^6$Li target [Fig. 1(a)] that there is a broad structureless continuum yield beginning at low $^6$Li excitation energy, while the spectra from the $^{12}$C and $SiO_2$ targets [Figs. 1(b) and (c), respectively] indicate small yields in this region. This was also true of the spectra obtained in the experiments with the $^{16}$O beam.

Data were taken for the $^6$Li + $^{16}$O systems because $^{16}$O does not have a strongly collective state like the $2^+$ state of $^{12}$C, whose strength might obscure the effects of coupling to the $3^+$ state of $^6$Li. A typical spectrum for this system is shown in Ref. 8. The inelastic cross sections measured for $^6$Li + $^{16}$O at $E_{c.m.} = 18.7$ MeV are for the excitation of the $3^+$ state in $^6$Li and the $3^-$, 6.13 MeV state of $^{16}$O. The large continuum yield in the $^{16}$O spectra made the reliable extraction of yields for the excitation of the $2^+$ state of $^6$Li in the $^{16}$O + $^6$Li experiments impossible.

It was possible, however, to obtain an estimate of the direct breakup cross section in all three cases investigated. The elastic and inelastic cross sections measured here have an absolute uncertainty of 7%. The elastic scattering data is much more extensive than previously published[12–15] data for $^6$Li scattering from $^{12}$C and $^{16}$O in this energy range. The forward angle oscillations were carefully mapped out and back-angle data were also measured to $\theta_{c.m.} \approx 170°$. The inelastic angular distributions for the excitation of the $2^+$(4.44 MeV) state in $^{12}$C are also very ex-

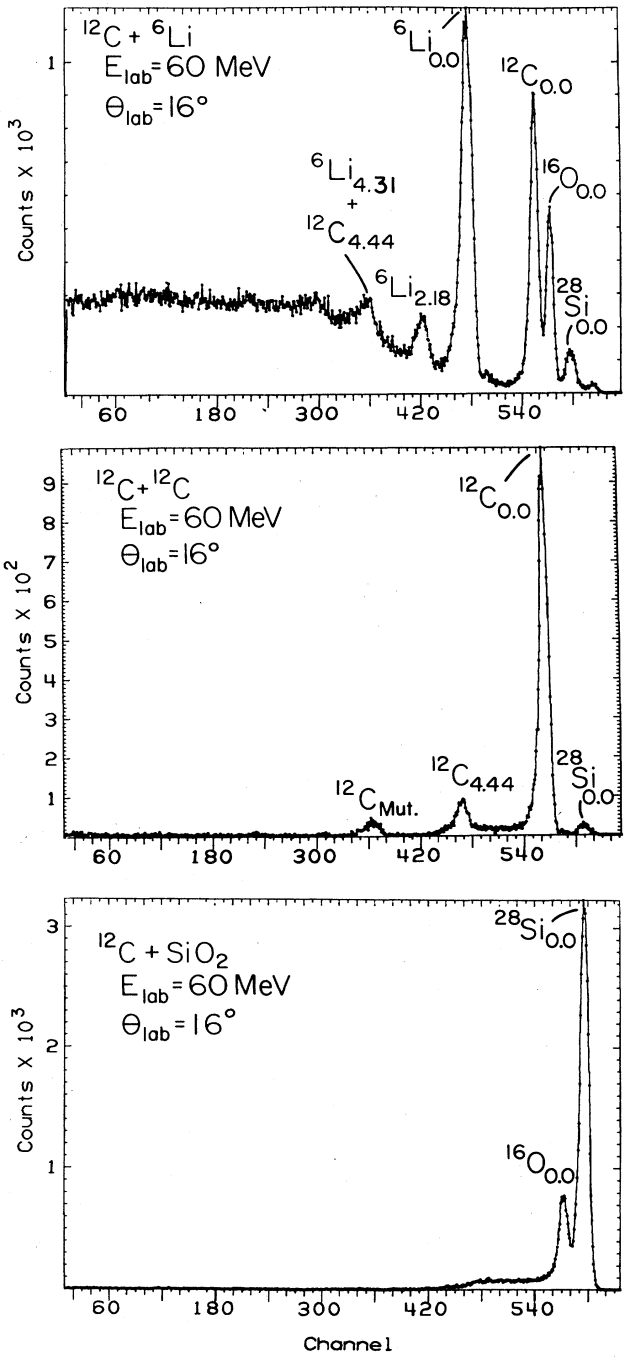


FIG. 1. Typical $^{12}$C linear energy spectra from the $^{12}$C + $^6$Li experiment taken on: (a) a $^6$Li target, (b) a $^{12}$C target, and (c) an $SiO_2$ target. The labeled peaks in the spectra correspond to the following reactions: $^{12}$C + $^6$Li elastic ($^6Li_{0.0}$) and inelastic scattering to the $3^+$($^6Li_{2.18}$) and $2^+$($^6Li_{4.31}$) states of $^6$Li as well as to the $2^+$($^{12}C_{4.44}$) state of $^{12}$C; $^{12}$C + $^{12}$C elastic ($^{12}C_{0.0}$) and elastic scattering for single ($^{12}C_{4.44}$) and mutual ($^{12}C_{mut}$) excitation of the $2^+$ state; $^{12}$C + $^{16}$O elastic scattering ($^{16}O_{0.0}$); and $^{12}$C + $^{28}$Si elastic scattering ($^{28}Si_{0.0}$). The peak labeled ($^6Li_{4.31}$: $^{12}C_{4.44}$) in spectrum (a) contains contributions from the excitation of both nuclei in the $^{12}$C + $^6$Li reaction.

tensive at both energies, and oscillate out of phase with the elastic scattering angular distributions. The inelastic data for the $0^+$(7.65 MeV) and $3^-$(9.64 MeV) states of $^{12}$C and the $3^-$(6.13 MeV) state of $^{16}$O are somewhat limited at forward angles, because the small cross sections made it difficult to extract the yields from the background. The inelastic angular distributions for the excitation of the $3^+$(2.18 MeV) state of $^6$Li show considerable structure, and oscillate out of phase with the elastic scattering angular distributions. The data for the excitation of the $2^+$(4.31 MeV) state of $^6$Li by $^{12}$C have a rather large error associated with them because the contribution from the excitation of the $2^+$(4.44 MeV) state of $^{12}$C with $^6$Li in its ground state had to be subtracted from the extracted yields.

An estimate of the continuum, or direct, breakup cross section was obtained at each angle by summing the continuum yield of the spectra for excitation of $^6$Li. The three angular distributions obtained in this way were structureless and forward peaked. A lower limit of the total continuum breakup cross section was obtained by integrating over angles. In this way, it was estimated that the total continuum breakup cross section is $>650$ mb for $^6$Li + $^{12}$C at 16 MeV, $>900$ mb for $^6$Li + $^{12}$C at 20 MeV, and $>1000$ mb for $^6$Li + $^{16}$O at 18.7 MeV.

## III. INELASTIC FORM FACTORS

The double-folding model[1] was employed to analyze the measured inelastic cross sections reported here. The real part of the nuclear form factor was calculated by folding the $M3Y$ interaction[2] with the transition density of the excited nucleus and the ground-state density of the other nucleus. The particular form of the $M3Y$ interaction used included a component to account for single-nucleon knockout exchange[16] and had the explicit form

$$v(r)=7999\frac{e^{-4r}}{4r}-2134\frac{e^{-2.5r}}{2.5r}-3908(r)\ . \tag{1}$$

The $^6$Li ground state density was obtained from the measured charge density of Suelzle *et al.*[17] by unfolding the proton charge distribution and assuming the neutron and proton densities to be identical. Harmonic oscillator densities were used for the target nuclei, and are given by

$$\rho_0(r)=(0.173+0.0647r^2)\exp(-0.352r^2) \tag{2}$$

for $^{12}$C, and

$$\rho_0(r)=(0.141+0.0647r^2)\exp(-0.298r^2) \tag{3}$$

for $^{16}$O. The proton charge distribution was also unfolded from these last two densities.

For simplicity, a derivative form was assumed for the $2^L$-pole radial transition densities $\rho_L^{ij}(r)$:

$$\rho_L^{ij}(r)=\delta_L^{ij}\left|\frac{d\rho_0(r)}{dr}\right|, \tag{4}$$

where $\rho_0(r)$ is the ground state density of the nucleus, and $\delta_L^{ij}$ is the $2^L$-pole nuclear deformation length for the coupling of the $i$th state to the $j$th state. The deformation length $\delta_L^{ij}$ for each transition ($i\rightarrow j$) was fixed by normalizing to the reduced electric transition probability, or $B(EL)$ value, through the relations

$$B(EL;KJ_i\rightarrow KJ_j)=\left|\langle J_iLKO\,|\,J_jK\rangle\frac{Ze}{A}\int_0^\infty\rho_L^{ij}(r)r^{L+2}dr\right|^2 \tag{5a}$$

for a rotational nucleus with band head $K$, and

$$B(EL;n_L=0\ J_i\rightarrow n_L=1\ J_j)=\left|\frac{Ze}{A}(2J_i+1)\int_0^\infty\rho_L^{ij}(r)r^{L+2}dr\right|^2 \tag{5b}$$

TABLE I. Deformation lengths for inelastic transitions in $^6$Li, $^{12}$C, and $^{16}$O.

| Nucleus | Transition ($i\rightarrow j$) | $Q$ (MeV) | $L$ | $B(EL)$ ($e^2$fm$^{2L}$) | $Q_{20}$ ($e$ fm$^2$) | $\lvert\delta_L^{ij}\rvert$ (fm) | $\lvert\delta_L^{ij}\rvert$ (fm) | $\delta_L^{ij}$ (fm) | $\delta_L^{ij}$ (fm) |
|---|---|---|---|---|---|---|---|---|---|
| $^6$Li | $1^+\rightarrow3^+$ | −2.18 | 2 | 25.6[a] | −0.64[b] | 1.88[c] | 1.54±0.2[d] | −1.54±0.2[e] | −0.78[f] |
| $^6$Li | $1^+\rightarrow2^+$ | −4.31 | 2 | 7.9[a] | −0.64[b] | 0.94 | 1.54±0.4 | −1.54±0.4 | −0.78 |
| $^{12}$C | $0^+\rightarrow2^+$ | −4.44 | 2 | 42[g] | −21.0[h] | 1.48 | 1.58±0.1 | −1.48±0.1 | −1.52 |
| $^{12}$C | $0^+\rightarrow3^-$ | −9.64 | 3 | 749[i] | | 1.91 | 1.29±0.1 | −1.29±0.1 | −1.52 |
| $^{16}$O | $0^+\rightarrow3^-$ | −6.13 | 3 | 1325[j] | | 1.55 | 1.55±0.1 | 1.41±0.1 | |

[a]Reference 22.
[b]Reference 27.
[c]These deformation lengths were determined from the $B(EL)$ values.
[d]These deformation lengths were determined from the present DWBA analysis.
[e]These deformation lengths were determined from the present coupled channels analysis.
[f]The reorientation deformation length was determined from $Q_{20}$ for $^{12}$C and was assumed to be $\delta_2^{ij}/2$ for $^6$Li.
[g]References 27 and 28.
[h]References 19 and 25.
[i]Reference 29.
[j]Reference 30.

for the excitation of a one-phonon mode in a vibrational nucleus. This procedure simply sets the charge and nuclear deformation lengths equal and assumes that the proton and neutron densities have the same shape. The experimental $B(EL)$ values were obtained from electron scattering and are given in Table I. Also in Table I are the deformation lengths derived using Eqs. (4) and (5). The normalization of the transition densities and the calculation of the double-folded form factors were performed with the computer code DFPOT.[18] In the DWBA and CC calculations the double-folded form factors were multiplied by the same renormalization factor $N$, as the double-folded optical potentials.

For the transitions in $^6$Li and $^{12}$C considered here, a rotational model was assumed and a deformed Woods-Saxon (WS) potential given by

$$W_L(r)=\int \frac{-iW_0 Y_{L0}(\hat{r})d\hat{r}}{1+\exp\{[r-R_I-\delta_L^{ij}Y_{LO}(\hat{r})]/a_I\}} \quad (6)$$

was used for the imaginary part of the form factors for a transition of multipolarity $L$. The same deformation lengths $\delta_L$ were used for both the real and imaginary form factors. The $0^+\rightarrow 2^+$ and $0^+\rightarrow 3^-$ transitions in $^{12}$C and the $L=2$, $1^+\rightarrow 3^+$ and $1^+\rightarrow 2^+$ transitions in $^6$Li were considered. In the CC analysis, $L=2$ reorientation terms were included with double-folded real and deformed WS imaginary form factors. In the rigid rotor model, the transition deformation length $\delta_L^{ij}$ and the reorientation deformation length $\delta_L^{jj}$ should be equal, but by allowing the two strengths to differ, one can compensate for possible defects of the model. Since the $L=2$ transitions in $^6$Li and $^{12}$C are very strong, we chose not to set $\delta_2^{jj}=\delta_2^{ij}$. Rather, for transitions in $^{12}$C, the reorientation quadrupole deformation length $\delta_2^{jj}$ was fixed by normalizing to the intrinsic electric quadrupole moment $Q_{20}$,[19,20] on which the ground state band is built, through the relation

$$\int_0^\infty \rho_2^{jj}(r)r^4dr=\frac{A}{Ze}\left[\frac{5}{16\pi}\right]^{1/2}Q_{20}\ . \quad (7)$$

The deformation length derived using the preceding equation is given in Table I and turned out to be almost equal to the deformation length for the $0^+\rightarrow 2^+$ transition derived using Eq. (5a) and the $B(E2)$ value. Since the quadrupole moment of $^6$Li is very small, the deformation length for the reorientation terms of this nucleus were simply assumed to be half the value of the deformation length for the $1^+\rightarrow 3^+$ transition.

The $3^-$ state in $^{16}$O is generally regarded as a vibrational state, and therefore the imaginary part of the form factor used here for the $0^+\rightarrow 3^-$ transition was a derivative WS given by

$$W(r)=\delta_3\frac{d}{dr}\frac{iW_0}{1+\exp[(r-R_I)/a_I]}\ . \quad (8)$$

The same octupole deformation length $\delta_3$, derived using the experimental $B(E3)$ value and Eq. (5b), was used for both the real and imaginary form factors.

In a previous paper[9] the elastic scattering data were analyzed with Woods-Saxon and double-folded potentials. The main results are summarized here. Several different Woods-Saxon potentials were found to fit each angular distribution well, although the fits to the 16-MeV $^6$Li + $^{12}$C data were of inferior quality to those for $^6$Li + $^{12}$C at 20 MeV and $^6$Li + $^{16}$O at 18.7 MeV. This could be related to the occurrence of a resonantlike structure[11] around $E_{\text{c.m.}}=15.2$ MeV in $^6$Li + $^{12}$C excitation function data. There was little difference between the new 20 MeV $^6$Li + $^{12}$C data and previously measured data[12] at 20.4 MeV, or between the optical potentials required to fit them, indicating that there is no rapid energy dependence at this energy. The double-folded potentials were calculated by convoluting the $M3Y$ effective nucleon-nucleon

TABLE II. Double folding real and Woods-Saxon imaginary potential parameters obtained from optical model and coupled channels calculations for the $^6$Li + $^{12}$C, $^{16}$O systems. The imaginary interaction radius is given by $R_I=r_I(A_p^{1/3}+A_T^{1/3})$, while that for the Coulomb interaction is given by $R_c=1.25$ $(A_p^{1/3}+A_T^{1/3})$.

| System | $E_{\text{c.m.}}$ (MeV) | Coupling[a] | $N$ | $W_0$ (MeV) | $r_I$ (fm) | $a_I$ (fm) |
|---|---|---|---|---|---|---|
| $^6$Li + $^{12}$C | 16 | OM | 0.71 | 6.77 | 1.34 | 0.59 |
| | | OM[b] | 0.69 | 7.85 | 1.34 | 0.62 |
| | | $^6$Li* | 0.85 | 9.80 | 1.13 | 0.70 |
| | | $^{12}$C* | 0.85 | 8.00 | 1.13 | 0.78 |
| $^6$Li + $^{12}$C | 20 | OM | 0.69 | 8.65 | 1.17 | 0.82 |
| | | $^6$Li* | 0.85 | 9.50 | 1.13 | 0.70 |
| | | $^{12}$C* | 0.85 | 9.00 | 1.13 | 0.78 |
| $^6$Li + $^{16}$O | 18.7 | OM | 0.61 | 6.62 | 1.35 | 0.80 |
| | | $^6$Li* | 0.75 | 10.9 | 1.07 | 0.78 |
| | | $^{16}$O* | 0.61 | 5.50 | 1.35 | 0.80 |

[a]Optical model fits are indicated as OM. $^6$Li*, $^{12}$C*, and $^{16}$O* denote, respectively, coupled-channels calculations in which excited states of $^6$Li, $^{12}$C, and $^{16}$O were included.
[b]Obtained by fitting forward angle data only and used in DWBA analysis.

interaction with the ground state densities of the projectile and target nuclei. The potentials needed to be reduced in strength by about 30% in order to reproduce the data. Similar quality fits were then obtained to those using Woods-Saxon potentials.

## IV. DWBA ANALYSIS

The distorted-wave Born approximation (DWBA) calculations were performed with the computer code CHUCK3.[21] The distorted waves were generated with the double-folded (DF) real and Woods-Saxon (WS) imaginary optical potentials which fitted the corresponding elastic data. These potentials are listed in Table II. Since the potential obtained by fitting the anomalous large angle 16 MeV $^6$Li + $^{12}$C data did not provide a good fit at forward angles, the forward angle data ($\theta_{c.m.} < 90°$) were fitted, starting with the 20 MeV potential parameters, and the resulting potential was used in the DWBA calculations at 16 MeV. Only the imaginary potential parameters were searched on during the fitting process and the final parameters are given in Table II. The real DF form factors were normalized by the same factor as the real potentials. Coulomb excitation contributions were included with the same deformation lengths, derived from the experimental $B(EL)$ values using Eqs. (4) and (5), as the nuclear form factors.

The results of the DWBA calculations for the $^6$Li + $^{12}$C data at 16 and 20 MeV are shown as the full lines in Figs. 2 and 3, respectively. Since the 16-MeV elastic-scattering

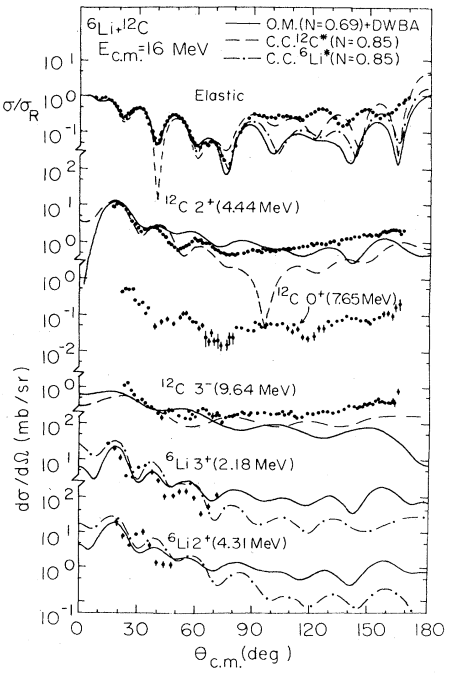


FIG. 2. Optical model plus DWBA (full lines), $^6$Li*-coupling CC (dash-dot lines), and $^{12}$C*-coupling CC (dashed lines) calculations for the 16 MeV $^6$Li + $^{12}$C data. Real double-folded and deformed Woods-Saxon imaginary form factors have been used.

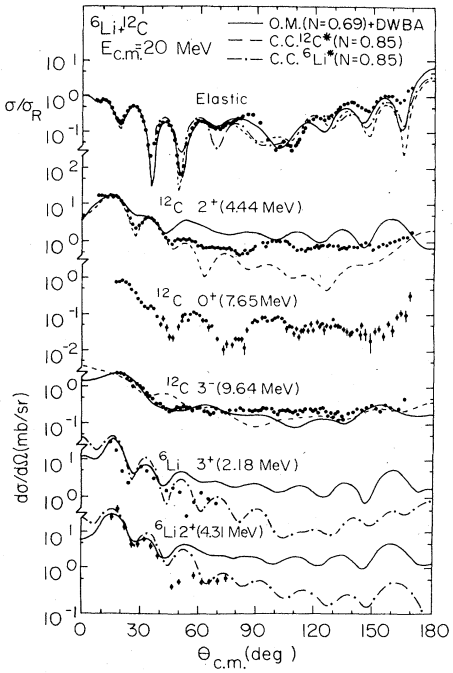


FIG. 3. Optical model plus DWBA (full lines), $^6$Li*-coupling CC (dash-dot lines), and $^{12}$C*-coupling CC (dashed lines) calculations for the 20 MeV $^6$Li + $^{12}$C data. Real double-folded and deformed Woods-Saxon imaginary form factors have been used.

data have contributions from mechanisms other than shape-elastic scattering, the DWBA analysis was first performed on the 20 MeV data and the results were then used in calculations for the 16 MeV data. The predictions for the excitation of the 2$^+$(4.44 MeV) and 3$^-$(9.64 MeV) states of $^{12}$C at 20 MeV reproduce the data well at forward angles with only slight adjustments of the deformation lengths (Table I), but are too large in magnitude at back angles.

Some attempts were made to describe the data for the excitation of the 0$^+$(7.65 MeV) state of $^{12}$C assuming a breathing-mode[20] excitation. This is basically an $L=0$ vibrational excitation. However, an acceptable description of the data could not be obtained. Since the cross sections for this state are small, and therefore should not have a large effect on the elastic scattering, it was not included in subsequent calculations. The predictions for the excitations of the 3$^+$(2.18 MeV) and 2$^+$(4.31 MeV) state of $^6$Li at 20 MeV have the proper far-forward angle magnitude and oscillatory structure, but overpredict the magnitude of the cross sections at the larger angles. It was necessary to reduce the deformation length for the $1^+ \rightarrow 3^+$ transition in $^6$Li by about 15—20% from the value derived using the $B(E2)$ value, while the deformation length for the $1^+ \rightarrow 2^+$ transition had to be increased by about 60%.

The results of the DWBA calculations for the $^6$Li + $^{16}$O data are shown as the full lines in Fig. 4. The 3$^-$(6.13 MeV) angular distribution is well reproduced without adjustment of the deformation length. The prediction for the 3$^+$(2.18 MeV) state of $^6$Li has the proper forward angle magnitude with the same adjustment of the

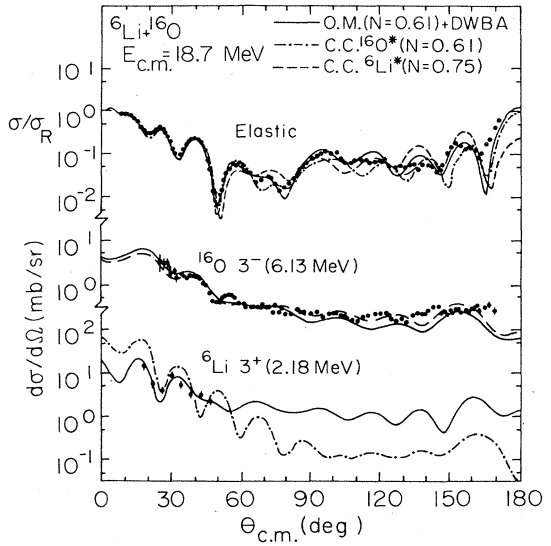


FIG. 4. Optical model plus DWBA (full lines), $^6$Li*-coupling CC (dash-dot lines), and $^{16}$O*-coupling CC (dashed lines) calculations for the 18.7 MeV $^6$Li + $^{16}$O data. Real double-folded and deformed Woods-Saxon imaginary form factors have been used.

deformation length as found necessary in the analysis of the $^{12}$C data.

## V. COUPLED-CHANNELS ANALYSIS

Coupled-channels (CC) calculations were performed to investigate the effect of coupling to the first-excited state of $^6$Li on the calculated elastic scattering angular distribution. The computer code CHUCK3,[21] which was used for these calculations, does not allow for the treatment of coupling to excited states of both nuclei. Therefore, for each system, two sets of calculations were performed, one for projectile coupling and the other for target coupling. In these calculations, the optical model parameters obtained from fitting the elastic scattering data and the deformation lengths from the DWBA analysis were used as starting values for fitting the elastic and inelastic cross sections. Coulomb excitation was also included as before.

The analysis was first performed on the $^6$Li + $^{16}$O data, since the first excited state of $^{12}$C is strongly excited and may have a large influence on the elastic channel, complicating the effect of the projectile coupling. First, CC calculations were performed for coupling to the $3^+$ state of $^6$Li. This coupling had a great affect on the elastic scattering prediction, causing it to be drastically out of phase with the data, even at far-forward angles. The parameters $N$, $W_0$, $r_I$, and $a_I$ were then optimized to describe the data, resulting in the final parameters labeled $^6$Li* for the $^6$Li + $^{16}$O system in Table II and the fits shown as the dash-dot lines in Fig. 4. The description of the elastic scattering data is reasonable over the whole angular range. The part from $\theta_{c.m.}=60°$–$90°$ was found to be very sensitive to reorientation effects in the $3^+$ state and requires a negative $\delta_2^{11}$ to be described correctly. The $3^+$ prediction has the correct forward angle magnitude with the same value of $|\delta_2^{01}|$ that was found in the DWBA analysis (Table I). Coupling to the $3^-$(6.13 MeV) state in $^{16}$O was then considered, again starting with the elastic scattering optical model parameters. The target state was found to affect only the large angle magnitude of the elastic scattering prediction. Simply by reducing the depth of the imaginary potential $W_0$ by about 20% resulted in the predictions shown as the dashed-dotted lines in Fig. 4 and the parameters of Table II. The descriptions of the elastic scattering and $3^-$ angular distributions are quite good over the entire angular range.

Calculations were then performed on the 20-MeV $^6$Li + $^{12}$C data, starting with inclusion of the $3^+$ state of $^6$Li. As in the calculations for the $^6$Li + $^{16}$O system, this state was found to have a large influence on the elastic scattering prediction. After performing a grid search on the normalization of the real double-folded potential, a good description of the data was obtained with $N=0.85$. Coupling to the $2^+$ state of $^6$Li was then included and resulted in only a slight deterioration of the elastic-scattering fit. The results are shown as the dash-dot lines in Fig. 3 and the CC parameters are given in Table II. The fit to the elastic scattering data is quite reasonable and the two inelastic angular distributions are well described. As in the calculations for the $^6$Li + $^{16}$O system, the midregion ($\theta_{c.m.}=60°$–$120°$) of the elastic scattering angular distribution was found to be very sensitive to reorientation effects in the $3^+$ state and required a negative $\delta_2^{11}$ to be described correctly. The effect of coupling to the target states was then investigated, and the inclusion of the $2^+$ state in $^{12}$C was found to have much the same affect on the elastic scattering prediction as the $3^+$ state of $^6$Li. The $N=0.85$ potential obtained in the projectile coupling calculations was found to provide a very good fit to both the elastic and $2^+$ angular distributions, with the quadrupole deformation length $\delta_2^{01}$ for $^{12}$C equal to the value obtained from the $B(EL)$ value. The best fit required only small changes in $W_0$ and $a_I$. The inclusion of the reorientation term had little effect on the calculation. Coupling to the $3^-$ state was then included, causing some deterioration in the elastic scattering fit. It was necessary to decrease the octupole deformation length $\delta_3^{02}$ for this transition by about 30% to match the forward-angle prediction to the data. The results are shown as the dashed lines in Fig. 3 and the CC parameters are given in Table II. The description of the elastic scattering data is good and the two inelastic angular distributions are well reproduced. The same calculations for projectile and target coupling were then performed for the 16-MeV data, resulting in the predictions shown as the dash-dot and dashed lines, respectively, in Fig. 2 with the parameters given in Table II.

## VI. DISCUSSION

The optical model (OM) and DWBA (solid lines), $^6$Li*-CC (dash-dot lines), and $^{12}$C*- or $^{16}$O*-CC (dashed lines) fits to the elastic and inelastic data are compared in Figs. 2, 3, and 4. The OM and both sets of CC calculations provide comparable descriptions of the elastic scattering data in all three cases. The CC predictions for the excita-

tion of $^6$Li have the proper magnitude at larger angles, which were overpredicted by the DWBA. The CC fit to the $3^-$ state of $^{16}$O is quite good over the whole angular range, as is the prediction for the $3^-$ state of $^{12}$C. The CC fit to the $2^+$ state of $^{12}$C is much improved over that of the DWBA, however, the magnitude at back angles is low.

The inclusion of coupling to the $3^+$ state of $^6$Li had a large influence on the calculated elastic scattering angular distributions for both targets. A comparison of the final CC parameters with those obtained in the OM analysis (Table II) reveals two important effects of coupling to this low-lying, strongly excited state. The first is a substantial increase in the normalization $N$ of the DF potential from 0.70 to 0.85 for the $^6$Li + $^{12}$C system and from 0.61 to 0.75 for the $^6$Li + $^{16}$O system. This reduces the discrepancy in the depth of the real DF potential necessary to describe the scattering of $^6$Li and other heavy-ion projectiles. The second effect is a reduction in the strength of the imaginary potential in the surface region. This provides evidence that at least part of the large phenomenological imaginary potential which often dominates $^6$Li scattering arises from coupling to excited states of $^6$Li. Coupling to the $2^+$ state of $^6$Li was found to have only a minor effect on the results of the calculations for the $^6$Li + $^{12}$C system.

The coupling of the target states for the two systems had very different results. The $3^-$ state of $^{16}$O was found to have very little influence on the elastic scattering calculations, while the $2^+$ state of $^{12}$C was found to have as large an effect as the $3^+$ state of $^6$Li. This result indicates that $L=2$ coupling to the elastic channel is important and not the particular state from which it arises. The inclusion of the $3^-$ state of $^{12}$C in the CC calculations made relatively little difference in the elastic scattering predictions.

In Table I, the deformation lengths derived using the experimental $B(EL)$ values are compared with those determined in the DWBA and CC analyses. It was necessary to reduce the magnitude of the deformation length for the $1^+\rightarrow 3^+$ transition in $^6$Li by 15—20% from the value derived using the $B(E2)$ value of Eigenbrod.[22] This reduction is consistent with the results of Yen *et al.*[23] and Petrovich *et al.*[24] in which the obtained $B(E2)$ values were 10—20% lower than those of Eigenbrod. A substantial increase in the $|\delta_2^{02}|$ for the $1^+\rightarrow 2^+$ transition in $^6$Li was found necessary. This suggests that there may be a considerable contribution from two-step processes in the excitation of the $2^+$ level in $^6$Li. The magnitude of the quadrupole deformation length $|\delta_2^{01}|$ for the $0^+\rightarrow 2^+$ transition in $^{12}$C determined in the DWBA analysis is 7% greater than that obtained from the $B(E2)$ value. However, the deformation length derived from the $B(E2)$ value provides the correct forward-angle magnitude of the $2^+$ CC prediction to the data. The $\delta_3^{02}$ for the $0^+\rightarrow 3^-$ transition in $^{12}$C determined from the DWBA and CC analyses is 30% lower than that found from the $B(E3)$ value, but the $\delta_3^{01}$ for $^{16}$O is consistent with the $B(E3)$ value for that transition.

The signs of the quadrupole deformation lengths $\delta_2$ for the $1^+\rightarrow 3^+$ transition in $^6$Li and the $0^+\rightarrow 2^+$ transition in $^{12}$C were determined unambiguously in the CC analysis. The mid-angular region of the elastic scattering angular distributions is particularly sensitive to reorientation effects in the $^6$Li $3^+$ state and requires a negative $\delta_2$ to be described correctly. The CC fits for the $2^+$ state of $^{12}$C shown in Figs. 2 and 3 are also for a negative quadrupole deformation length. When the sign of $\delta_2^{01}$ for $^{12}$C was made positive, the CC elastic and $2^+$ predictions did not fit the data as well as with negative $\delta_2^{01}$. This was expected, since the intrinsic quadrupole moment $Q_{20}$ (Refs. 19 and 25) of $^{12}$C is negative. Changing the signs of the other deformation lengths had only minor effects on the results of the calculations. Therefore, negative deformation lengths were assumed for all other transitions, except for the octupole deformation length $\delta_3^{01}$ for the $0^+\rightarrow 3^-$ transition in $^{16}$O, which was taken to be positive by convention for a vibrational excitation.

As found in other studies of inelastic $^6$Li scattering, the real part of the transition form factor contributes relatively little in the inelastic cross sections in the DWBA. Setting the imaginary part of the form factor equal to zero reduced the cross sections by almost a factor of 10, while setting the real part equal to zero reduced the cross sections by only a factor of 2—4. Therefore, the inelastic cross sections are dominated by the imaginary form factor. The inelastic cross sections have significant contributions from the Coulomb form factor only at far-forward angles.

The overall results of the present calculations are not altered when different transition densities are used. DWBA and CC calculations performed using double-folded form factors generated with the microscopic transition densities of Kamimura[19] and Bassel *et al.*[26] for transitions in $^{12}$C and that of Petrovich *et al.*[24] for the $1^+\rightarrow 3^+$ transition in $^6$Li yielded results that were essentially identical to those presented here.

The coupled channels calculations presented in this paper have considered only excitations in the target or projectile. It would be desirable to execute calculations in which the excited states of both nuclei are coupled in a single calculation. These, however, involve a prohibitively large amount of computing time. For example, using our SEL 32/77 computer, a calculation coupling in states of $^6$Li and $^{12}$C simultaneously takes in excess of 10 h of CPU time, compared with about 30 min when only states in $^6$Li are considered, and about 10 min for states in $^{12}$C only. Preliminary calculations with an extended version of CHUCK, coupling states of both nuclei do not significantly alter the conclusions reached in this paper. In these calculations the value of $N$ does not change from those in which only states in $^6$Li are considered (i.e., those calculations denoted by $^6$Li*). A small change in the strength of the imaginary potential is observed. In particular, simultaneously coupling the $3^+$ state in $^6$Li and the $2^+$ state in $^{12}$C (which alone have a large effect on the elastic scattering) produces results very similar to those obtained in this paper.

## VII. CONCLUSIONS

Angular distributions have been measured for the elastic and inelastic scattering to states in both nuclei in the

$^6$Li + $^{12}$C reaction at $E_{c.m.} = 16$ and 20 MeV, and the $^6$Li + $^{16}$O reaction at $E_{c.m.} = 18.7$ MeV. The cross sections presented here for the excited states of $^6$Li are the first measurements for the excitation of the discrete unbound states of $^6$Li in a predominantly nuclear heavy-ion collision.

The inelastic scattering data were analyzed using both the DWBA and coupled-channels techniques with folded real and phenomenological imaginary form factors, with the deformation lengths taken from electron scattering. The DWBA provided quite reasonable descriptions of the forward angle inelastic data.

The coupled-channels predictions for the elastic scattering data provide quite reasonable descriptions of the data, with better fits at large angles then obtained with the optical model. The coupled-channels predictions for the inelastic data provide a better description of the angular distributions than the DWBA, particularly at large angles. The deformation lengths obtained in the coupled-channels analysis are in good agreement with those obtained in the DWBA analysis.

Coupled-channels effects due to the $3^+$ state of $^6$Li are very important in the scattering of $^6$Li projectiles. When coupling to this low-lying, strongly excited state was taken into account, two important results were observed. The first being that the normalization of the real double-folded potential, necessary to fit the elastic scattering data, was significantly closer to unity for both targets, thus reducing the discrepancy between $^6$Li and other heavy-ion projectiles. The second being that a comparison of the imaginary potentials obtained from the OM and CC fits shows that when the coupling is included the imaginary potential becomes weaker in the surface region. This provides evidence that at least part of the large phenomenological imaginary potential which often dominates $^6$Li scattering arises from coupling to excited states of the $^6$Li projectile. The $2^+$ state in $^6$Li, and the $3^-$ states in $^{12}$C and $^{16}$O were found to be relatively unimportant. Coupling to the $2^+$ state of $^{12}$C was found to have much the same effect on the elastic scattering prediction as coupling to the $3^+$ state of $^6$Li. This result shows that it is the total $L=2$ strength that matters, rather than the specific nuclear state with which it is associated.

Also, from the present work, it was estimated that the total continuum breakup cross section was $\geq 650$ mb for $^6$Li + $^{12}$C at 16 MeV, $\geq 900$ mb for $^6$Li + $^{12}$C at 20 MeV, and $\geq 1000$ mb for $^6$Li + $^{16}$O at 18.7 MeV. This is very much larger than the total inelastic cross sections for the $3^+$ state ($\sigma_{\text{tot}(3^+)} \approx 24$, 27 and 30 mb for $^6$Li + $^{12}$C at 16 and 20 MeV, and $^6$Li + $^{16}$O at 18.7 MeV, respectively) obtained from the coupled-channels calculations, and it is possible that, if the continuum breakup could be included in coupled-channels calculations, the normalization discrepancy of the real double-folded potential might be removed. The theoretical work of Ref. 3 is concerned with this, and the data presented here for the excitation of $^6$Li should be valuable in the context of understanding breakup effects in elastic scattering.

## ACKNOWLEDGMENTS

We wish to acknowledge many helpful discussions with F. Petrovich and D. Robson. We are grateful for the support of this work provided by the National Science Foundation and the State of Florida.

*Present address: Argonne National Laboratory, Argonne, IL 60439.

†Present address: Department of Physics, University of Petroleum and Minerals, Dhahran, Saudi Arabia.

[1]G. R. Satchler and W. G. Love, Phys. Rep. **55**, 183 (1979); J. Cook and K. W. Kemper, Arab. J. Sci. Eng. **8**, 331 (1983); and references therein.

[2]G. Bertsch, J. Borysowicz, H. McManus, and W. G. Love, Nucl. Phys. **A284**, 399 (1977).

[3]I. J. Thompson and M. A. Nagarajan, Phys. Lett. **106B**, 163 (1981); Y. Sakuragi, M. Yahiro, and M. Kamimura, Prog. Theor. Phys. **68**, 322 (1982); **70**, 1047 (1983).

[4]H. W. Wittern, Phys. Lett. **32B**, 441 (1970).

[5]A. C. Shotter, A. N. Bice, J. M. Wouters, W. D. Rae, and J. Cerny, Phys. Rev. Lett. **46**, 12 (1981).

[6]A. S. Goldhaber and H. H. Heckman, Ann. Rev. Nucl. Sci. **28**, 161 (1978).

[7]D. Scholz, H. Gemmeke, L. Lassen, R. Ost, and K. Bethge, Nucl. Phys. **A288**, 351 (1977).

[8]M. F. Vineyard, K. W. Kemper, and J. Cook, Phys. Lett. **142B**, 249 (1984).

[9]M. F. Vineyard, J. Cook, K. W. Kemper, and M. N. Stephens, Phys. Rev. C **30**, 916 (1984).

[10]W. Weiss, P. Egelhof, K. D. Hildenbrand, D. Kasser, M. Makowska-Rzeszutko, D. Fick, H. Ebinghaus, E. Steffens, A. Amakawa, and K.-I. Kubo, Phys. Lett. **61B**, 237 (1976).

[11]B. R. Fulton and T. M. Cormier, Phys. Lett. **97B**, 209 (1980).

[12]V. I. Chuev, V. V. Davydov, B. G. Novatskii, A. A. Oglobin, S. B. Sakuta, and D. N. Stepanov, J. Phys. (Paris) **32**, C6, 161 (1971).

[13]K. Bethge, K. Meier-Ewert, and K. O. Pfeiffer, Z. Phys. **208**, 486 (1968); P. Schumacher, N. Ueta, H. H. Duhm, K.-I. Kubo, and W. J. Klages, Nucl. Phys. **A212**, 573 (1973).

[14]G. Bassani, N. Saunier, B. M. Traore, J. Raynal, A. Foti, and G. Pappalardo, Nucl. Phys. **A189**, 353 (1972).

[15]P. K. Bindal, K. Nagatani, M. J. Schneider, and P. D. Bond, Phys. Rev. C **9**, 2154 (1974).

[16]M. Golin, F. Petrovich, and D. Robson, Phys. Lett. **64B**, 253 (1976).

[17]L. R. Suelzle, M. Y. Yearian, and H. Crannell, Phys. Rev. **162**, 992 (1967).

[18]J. Cook. Comput. Phys. Commun. **35**, 125 (1982).

[19]M. Kamimura, Nucl. Phys. **A351**, 456 (1981); W. J. Vermeer, M. T. Estat, J. A. Kuehner, R. H. Spear, A. M. Baxter, and S. Hinds, Phys. Lett. **122B**, 23 (1983).

[20]H. Uberall, *Electron Scattering from Complex Nuclei* (Academic, New York, 1971).

[21]P. D. Kunz (unpublished) (with modifications by J. R. Comfort).

[22]F. Eigenbrod, Z. Phys. **228**, 337 (1969).

[23]R. Yen, L. S. Cardman, D. Kalivisky, J. R. Legg, and C. K. Bockelman, Nucl. Phys. **A235**, 135 (1974).

[24]F. Petrovich, R. H. Howell, C. H. Poppe, S. M. Austin, and G. M. Crawley, Nucl. Phys. **A383**, 355 (1982).

[25]G. Ripka, Adv. Nucl. Phys. **1**, 183 (1968); A. Nakada, Y. Tomzuka, and Y. Horikawa, Phys. Rev. Lett. **27**, 745 (1971).
[26]R. H. Bassel, B. A. Brown, R. Lindsay, and N. Rowley, J. Phys. G **8**, 1215 (1982).
[27]F. Ajzenberg-Selove, Nucl. Phys. **A320**, 1 (1979).
[28]P. H. Stelson and L. Grodzins, Nucl. Data Tables **1A**, 1 (1965).
[29]H. Crannell, Phys. Rev. **148**, 1107 (1966); P. Strehl and T. H. Schucan, Phys. Lett. **27B**, 641 (1968); H. Crannell, J. T. O'Brien, and D. I. Sober, *Proceedings of International Conference on Nuclear Physics with Electromagnetic Interactions, Mainz, 1979,* edited by H. Arenhovel and D. Drechsel (Springer, Berlin, 1979).
[30]A. M. Bernstein, Adv. Nucl. Phys. **3**, 325 (1969).